LU TP 16-63
December 2016

The landscape of $W^{\pm}$ and Z bosons produced in pp collisions up to LHC energies

Eduardo Basso

Instituto de Física, Universidade de São Paulo, Caixa Postal 66318,
05315-970 São Paulo, SP, Brazil

Claude Bourrely

Aix Marseille Univ, Univ Toulon, CNRS, CPT, Marseille, France

Roman Pasechnik

Department of Theoretical Physics,
Lund University, SE 223-62 Lund, Sweden

Jacques Soffer

Physics Department, Temple University,
1925 N, 12th Street, Philadelphia, PA 19122-1801, USA

Abstract

We will consider a selection of recent experimental results on electroweak $W^{\pm}$, Z gauge boson production in pp collisions at BNL RHIC and CERN LHC energies. We will study various aspects of these data and they will be compared to the predictions of perturbative QCD calculations, based on different sets of parton distribution functions. We will also propose some new tests for future data taking.

Key words: electroweak gauge bosons; Drell-Yan process; parton distribution functions.

1 Introduction

The ongoing measurements at particle colliders such as RHIC and the LHC continue precision tests of particle production mechanisms. In this respect, there is a growing demand for a better understanding of underlined QCD uncertainties, in particular, related to modeling of parton density functions (PDFs), the key ingredients of QCD collinear factorisation. A major effort of the Particle Physics community over past decades has been directed towards constraining the QCD parton (quark and gluon) dynamics at various momentum scales connected, via DGLAP evolution, to the universal nonperturbative parton densities at some low scale Q_0. The latter are not fully predicted by the first QCD principles but are usually parameterised and extracted from the data.

In recent years, production of electroweak gauge bosons, both charged ($W^{\pm}$) and neutral (Z^0, γ^*), has attracted a lot of attention from theory and experiments as an important test of QCD (see e.g. Refs. [1, 2, 3]). In particular, these processes are traditionally considered as an ideal tool for probing PDFs at various x and Q^2 [4, 5, 6]. For example, by controlling the c.m.s. energy $\sqrt{s}$, di-lepton rapidity Y and invariant mass M in the Drell-Yan (DY) process $pp \to (Z^0/\gamma^* \to l^+l^-) + X$ one could access quark and gluon PDFs at both small and large $x_i = (M/\sqrt{s})e^{\pm Y}$ with $i = 1, 2$ denoting the incoming protons. While contributions from gluon and sea-quark PDFs to gauge boson production dominate presumably in kinematic regions of the LHC (except, probably, highly forward regions of the phase space), at lower energies of RHIC one expects an increased sensitivity to valence quark distributions.

In our previous study [7], several most recent PDF parameterizations at the next-to-leading order (NLO) including the statistical PDF (known as NLO BS15) model [8] were used for a description of the existing DY data for the differential distributions available from Tevatron and LHC measurements. While a fairly good description of the DY data at high energies has been found for all the chosen PDF sets, at low energies the PDF models exhibit more substantial differences in shapes of the invariant mass and x_F distributions. Provided that the BS15 model having much fewer free parameters results in as good data description as other popular models so it should be considered on the same footing as the current global PDF fits. In this Letter, we extend our previous analysis [7] to RHIC and LHCb kinematic regions as well as incorporate $W^{\pm}$ production observables.

The paper is organized as follows. In Section 2, we review the main features of two sets of PDFs we have used for our calculations. In Section 3, we consider a selection of recent $W^{\pm}$ production data sets available from STAR, CMS and LHCb and the DY-pair $Z/\gamma^* \to l\bar{l}$ production data – from the STAR and LHCb measurements. We make a comparison of theoretical predictions for the selected PDFs with these data. We give our summary and final remarks in Section 4.

2 Selection of two PDF sets

We will now summarize the essential properties of two sets of PDFs which will be tested in our further analysis of $W^{\pm}$ and DY-pair production in pp collisions at various energies.

The basic features of the statistical PDF approach alternative to canonical polynomial parameterizations which are inspired by the Regge theory at small x and by counting rules at large x have been discussed in Ref. [8]. In particular, (anti)quark distributions at the input scale $Q_0^2 = 1\,\mathrm{GeV}^2$

$$xq^h(x,Q_0^2) = \frac{A_q X_{0q}^h x^{b_q}}{\exp[(x - X_{0q}^h)/\bar{x}] + 1} + \frac{\tilde{A}_q x^{\tilde{b}_q}}{\exp(x/\bar{x}) + 1}\,, \tag{1}$$

$$x\bar{q}^h(x,Q_0^2) = \frac{\bar{A}_q (X_{0q}^{-h})^{-1} x^{b_{\bar{q}}}}{\exp[(x + X_{0q}^{-h})/\bar{x}] + 1} + \frac{\tilde{A}_q x^{\tilde{b}_q}}{\exp(x/\bar{x}) + 1}\,, \tag{2}$$

are defined in terms a quasi Fermi-Dirac function (first terms) and a helicity independent diffractive component (second terms). Note, the latter does not enter the quark helicity Δq and valence $q - \bar{q}$ distributions. The multipliers X_{0q}^h and $(X_{0q}^{-h})^{-1}$ in the diffractive contributions have been justified in the statistical approach to transverse momentum dependent PDFs in Ref. [9]. In Eqs. (1) and (2) for a given quark q with fixed helicity $h = \pm$ the parameters $\bar{x}$ and X_{0q}^h play the role of universal temperature and thermodynamical potential encoding the main characteristics of the model (for antiquarks the sign of helicity and potentials is changed). Remarkably, the statistical PDF approach enables to describe both upolarised observables and helicity asymmetries. In what follows, however, only spin-independent observables are considered.

The statistical (anti)quark distributions contain in total eight parameters[1]

[1]It turns out that X_{0u}^- and X_{0d}^- were found almost identical.

for a given q, namely, $\bar{A}_q$, A_q, $\tilde{A}_q$, $X^{\pm}_{0q}$, $\bar{b}_q$, b_q, and $\tilde{b}_q$. Then, the valence sum rule,

$$\int (q(x) - \bar{q}(x))dx = N_q\,, \qquad N_q = 2, 1, 0$$

for u, d, s quarks, respectively, reduces the parameter space to seven free parameters. The additional constraints apply for $q = \{u, d\}$ [10]

$$\bar{A}_u = \bar{A}_d\,, \quad A_u = A_d\,, \quad b_u = b_d\,, \quad \tilde{A}_u = \tilde{A}_d\,, \quad \tilde{b}_u = \tilde{b}_d\,, \quad \bar{b}_u = \bar{b}_d\,, \qquad (3)$$

thus, leading to eight free parameters in the sector of light quarks such that the diffractive contribution is flavor independent (for more details, see e.g. Ref. [11]). The expression for the statistical gluon PDF at $\mu = Q_0$ is inspired by the black-body spectrum and has a form of a quasi Bose-Einstein function

$$xG(x, Q_0^2) = \frac{A_G x^{b_G}}{\exp(x/\bar{x}) - 1}\,, \qquad (4)$$

where A_G is found by the momentum sum rule such that b_G is the only additional free parameter.

To conclude, the statistical PDF sets[2] contain *seventeen* free parameters in total. Besides the temperature $\bar{x}$ and the exponent of the gluon distribution b_G, the light u, d and strange s quark PDFs are constructed in terms of *eight* and *seven* free parameters, respectively. These were fitted to a large set of accurate unpolarised and polarised DIS data *only* at the NLO QCD level and therefore are denoted as NLO BS15 from now on.

Let us discuss the second PDF set used in our calculations of the unpolarized cross sections below. Several versions were proposed by the CTEQ-TEA global analysis of QCD up to NNLO [12] including data from HERA, Tevatron and LHC. For each flavor the Regge-motivated parameterisation is of the form

$$xf_a(x, Q_0^2) = x^{a_1}(1 - x)^{a_2} P_a(x)\,, \qquad (5)$$

with a slowly-varying polynomial factor $P_a(x)$. In the CT14 model [13] this factor for valence distributions is represented in terms of a linear combination

[2]In Ref. [8] we have also considered the helicity gluon distribution which is irrelevant in the present work.

of Bernstein polynomials

$$
\begin{aligned}
&P_{q_v} = d_0 p_0(y) + d_1 p_1(y) + d_2 p_2(y) + d_3 p_3(y) + d_4 p_4(y)\,, \qquad y = \sqrt{x}\,,\\
&p_0(y) = (1-y)^4\,,\ p_1(y) = 4y(1-y)^3\,,\ p_2(y) = 6y^2(1-y)^2\,,\\
&p_3(y) = 4y^3(1-y)\,,\ p_4(y) = y^4\,.
\end{aligned} \tag{6}
$$

By fixing $d_1 = 1$, $d_3 = 1 + a_1/2$ and using the valence sum rule the number of free parameters for each flavor is reduced to four. Thus, eight parameters fully determine the valence u_v and d_v distributions. Due to fewer constraints on the gluon distribution, the CT14 gluon PDF is constructed in terms of a lower-order polynomial

$$
\begin{aligned}
&P_g(y') = g_0\left[e_0 q_0(y') + e_1 q_1(y') + q_2(y')\right]\,, \quad q_0(y') = (1-y')^2\,,\\
&q_1(y') = 2y'(1-y')\,, \quad q_2(y') = {y'}^2\,,
\end{aligned} \tag{7}
$$

where $y' = 1-(1-\sqrt{x})^2 = 2\sqrt{x}-x$. With an account for the momentum sum rule the gluon PDF is determined by five free parameters in total. Fourth-order polynomials in the same variable y' as for the gluon PDF were employed for building the sea $\bar{d}$ and $\bar{u}$ distributions assuming $\bar{u}(x)/\bar{d}(x) \to 1$ at $x \to 0$. Altogether, in the CT14 model the sectors of valence and sea quark PDFs contain *eight* and *thirteen* free parameters, respectively, while the gluon PDF contains *five* parameters amounting to *twenty six* fitting parameters in total. The (N)NLO QCD global fits in this model have been performed at Q_0=1.295 GeV.

In numerical analysis we employ the up-to-date computing tools available for high precision PDFs studies. All the numerical results presented below were obtained using the `DYRes` code [14] which computes the DY observables up to NNLO performing the resummation of logarithms that become large when the vector boson transverse momentum is much smaller than the boson mass. Such a resummed result is matched order by order, up to $\mathcal{O}(\alpha_s^2)$, with the fixed-order result at large transverse momenta which is obtained within the dipole formalism [15] and is implemented in the `MCFM` code [16, 17]. The divergences in the fixed-order calculation at small p_T are subtracted resulting in a modification of the `DYNNLO` program [18] which was used in our previous DY analysis [7]. As an important test of our calculations, with appropriate constraints the `DYRes` results are in overall agreement with the `DYNNLO` ones as expected, with an exception that `DYNNLO` results on the W^+/W^- ratio appear to describe the current LHCb data better than the `DYRes` ones.

3 Results for $W^{\pm}$ and Z/γ^* observables

Consider first, as displayed in Fig. 1, a comparison of preliminary STAR data [19] on the W^+ to W^- differential cross section ratio

$$W^+/W^- \equiv \frac{d\sigma^+(\eta_e)/d\eta_e}{d\sigma^-(\eta_e)/d\eta_e}$$

with theoretical predictions based on the BS15 and CT14 PDF models. It is clear that both PDFs are consistent with the trend of the data given its poor uncertainty, but the planned 2017 run at BNL RHIC will be able to increase substantially the precision on this measurement. We observe that both predictions are almost sitting on top of each other, but they would be more distinguishable for larger η_e. However, this region is not accessible to STAR and the only way to find out which one agrees best with the data is to measure the individual cross sections near $\eta_e = 0$. This is indeed what one sees clearly in Fig. 2, where the BS15 result remains below the CT14 one in both W^+ and W^- cases. The K-factors were not applied for these observables since the data and theoretical calculations of the corresponding NNLO corrections are not yet available. We urge the STAR Collaboration to perform this important test.

The individual $W^{\pm}$ differential cross sections have been measured at the LHC at $\sqrt{s} = 8\,\text{TeV}$ by the CMS Collaboration [20] and are shown in Fig. 3 together with the corresponding theoretical predictions using the BS15 and CT14 PDF models. We notice an overall agreement in shapes of the W^+ cross section for both BS15 and CT14 predictions. However, the shape of the BS15 prediction for the W^- cross section somewhat deviates from the data in the high η_μ region. Both BS15 and CT14 predictions require a multiple K-factor ($K = 1.2$ for BS15 and $K = 1.03$ for CT14) to fit the data on the total cross section which should account (at least, partly) for the missing NNLO effects in these observables. The resulting K-factor for BS15 has turned out to be larger due to the fact that no LHC data was included in the fit of such parameterization which should be done in future studies.

Another way to present the data is the charge asymmetry defined as

$$\frac{d\sigma^+(\eta_\mu)/d\eta_\mu - d\sigma^-(\eta_\mu)/d\eta_\mu}{d\sigma^+(\eta_\mu)/d\eta_\mu + d\sigma^-(\eta_\mu)/d\eta_\mu},$$

which is related to W^+/W^- ratio considered above. This is shown in Fig. 4 (left), but the disagreement of the BS15 and CT14 predictions with the data

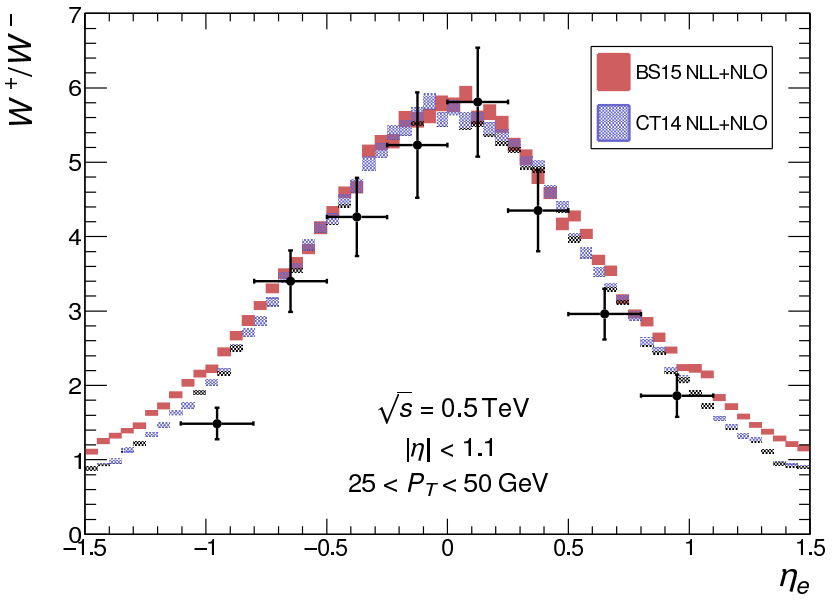

Figure 1: The ratio the W^+ and W^- differential cross sections at $\sqrt{s} = 500\,\text{GeV}$, versus the pseudo-rapidity of the charged lepton η_e, obtained with the BS15 and CT14 PDF models and compared to the preliminary data from the STAR experiment [19].

persists for a limited η region. In Fig. 4 (right) we present the predictions for W^+/W^- ratio at $\sqrt{s} = 13\,\text{TeV}$. This ratio was also measured at $\sqrt{s} = 8\,\text{TeV}$ in a large pseudo-rapidity region by the LHCb Collaboration [21] (see Fig. 5).

Several important aspects of the available data on Z/γ^* production have already been studied in our earlier paper [7]. In addition, in Fig. 6 we show the predictions using the BS15 and CT14 PDFs for the differential cross section for Z/γ^* production, versus the dilepton rapidity, in view of a future data taking from STAR at BNL RHIC. Once again it is not possible to distinguish them in this limited kinematic region, but it is a worthwhile experimental test to be done. Finally, in Fig. 7, we display the normalized differential cross sections for the forward Z/γ^* production from the LHCb experiment at two different energies ($\sqrt{s} = 8\,\text{TeV}$ [21] and $\sqrt{s} = 13\,\text{TeV}$ [22]) which turn out to be in a very good agreement with the predictions using

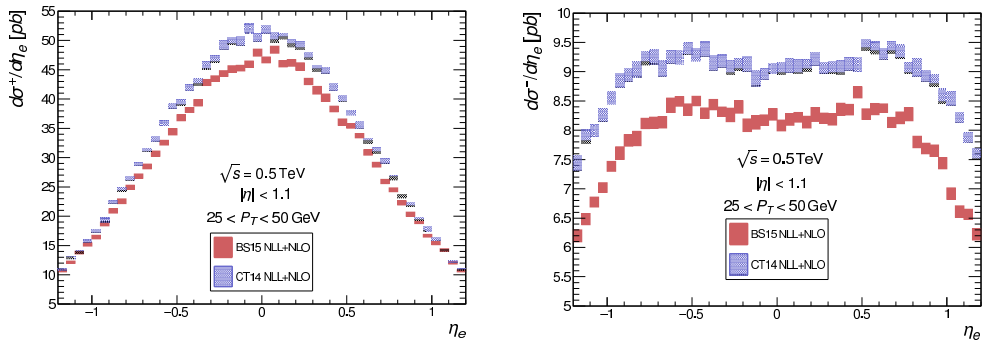

Figure 2: The differential cross sections for W^+, $d\sigma^+(\eta_e)/d\eta_e$ (left), and W^-, $d\sigma^-(\eta_e)/d\eta_e$ (right), production at $\sqrt{s} = 500\,\text{GeV}$, versus pseudo-rapidity of the charged lepton η_e, with the cuts corresponding to the acceptance of the STAR detector, as predicted by the BS15 and CT14 PDF models. No K-factors were applied here.

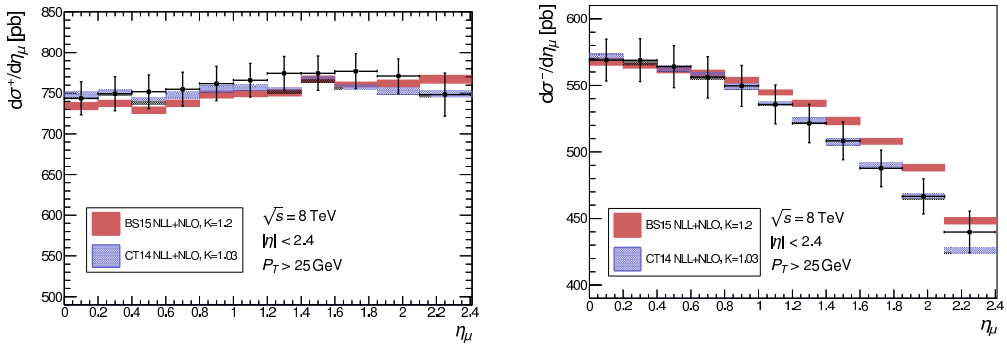

Figure 3: The differential cross sections for W^+, $d\sigma^+(\eta_\mu)/d\eta_\mu$ (left), and W^-, $d\sigma^-(\eta_\mu)/d\eta_\mu$ (right), production at $\sqrt{s} = 8\,\text{TeV}$, versus pseudo-rapidity of the charged lepton η_μ, with the cuts corresponding to the acceptance of the CMS detector, as predicted by the BS15 and CT14 PDF models (with $K = 1.2$ for BS15 and $K = 1.03$ for CT14), in comparison to the data by CMS Collaboration [20].

the BS15 and CT14 PDF models.

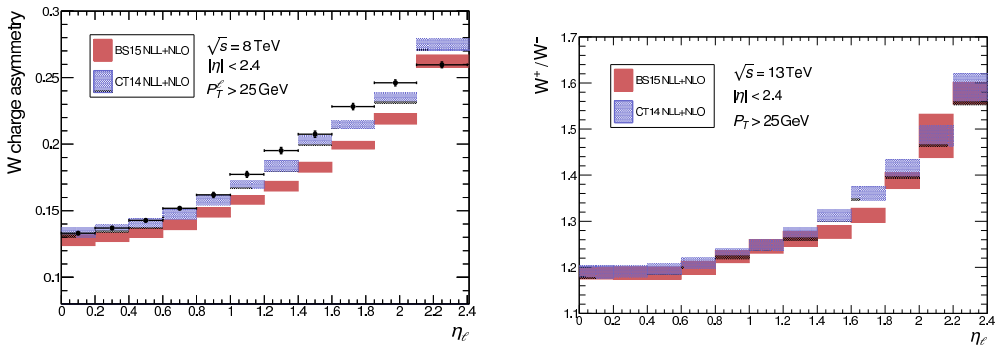

Figure 4: The $W^{\pm}$ charge asymmetry at $\sqrt{s} = 8\,\text{TeV}$, versus pseudo-rapidity of the charged lepton η_μ, with the cuts corresponding to the acceptance of the CMS detector, as predicted by the BS15 and CT14 PDF models, is shown in the left panel in comparison to the data by CMS Collaboration [20]. The prediction for W^+/W^- ratio based on BS15 and CT14 PDF models at $\sqrt{s} = 13\,\text{TeV}$ are shown in the right panel.

4 Summary

In this Letter, we have studied the $W^{\pm}$ charge asymmetry and the differential (in lepton pseudorapidity) $W^{\pm}$ cross sections, as well as the DY-pair $Z/\gamma^* \to l\bar{l}$ production cross section differential in dilepton rapidity, at RHIC ($\sqrt{s} = 500\,\text{GeV}$) and LHC ($\sqrt{s} = 8, 13\,\text{TeV}$) energies. In our analysis, we have used two distinct PDF sets at the NLO accuracy – the statistical BS15 model and the CTEQ CT14 parametrization. The corresponding predictions are compared to the most recent data sets and result in a fair description of a broad range of $W^{\pm}$ and Z/γ^* production data available from RHIC and the LHC. While the BS15 and CT14 PDF models predict very similar shapes of the differential cross sections, they require somewhat different K-factors correcting an overall normalisation.

No significant deviations between the NLO pQCD predictions using these PDFs parametrizations and the data have been found for the normalised Drell-Yan cross section at the LHC (see also Ref. [7]). A few minor deviations were found in $W^{\pm}$ observables. While the BS15 and CT14 PDF models predict similar shapes of the W^+ differential cross section, they require somewhat different K-factors correcting an overall normalisation. In the case of W^- production, the BS15 predictions lies somewhat above the CMS data

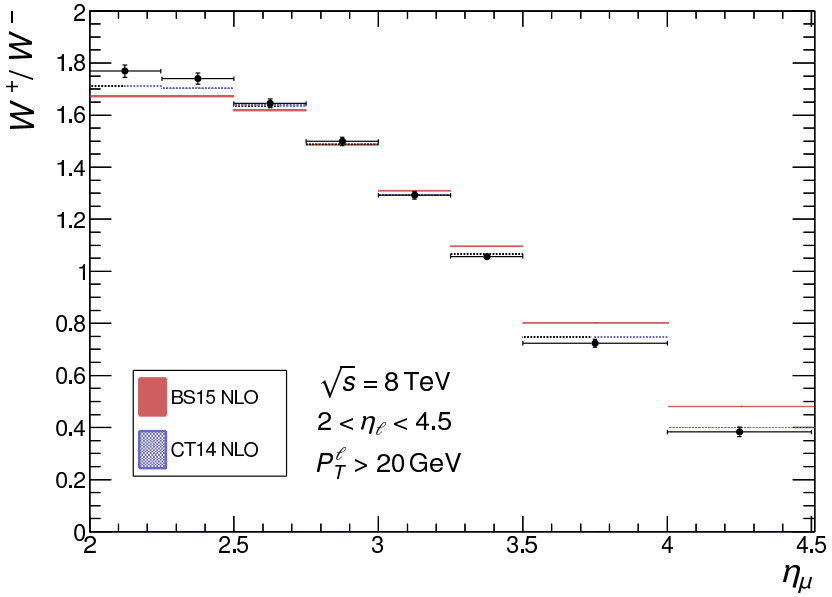

Figure 5: The W^+/W^- ratio based on BS15 and CT14 PDF models at $\sqrt{s} = 8$ TeV in comparison to the data from the LHCb Collaboration [21].

on $d\sigma/d\eta_\mu$ in the lepton rapidity range $\eta_\mu = 1 - 2$ which is due to the fact that the starting BS15 parameterisations were fitted to the DIS data only and have not been included into the global fits yet. The W^+/W^- ratio exhibit an overall consistency with the STAR and LHCb data but runs below the CMS data for both PDF models. A few minor deviations remain to be understood by a proper accounting for NNLO and resummation effects in a future study.

Clearly, our analysis indicates that in order to improve on precision of the data description the BS15 should be eventually included into global PDF fits. But provided that both PDF sets lead to similar results for vector boson production at the various energies, we would like to emphasize that the NLO BS15 model having much smaller number of free parameters extracted only from DIS is not significantly worse than other recent PDF parametrizations, which are fitted to much larger data sets, and can be used on the same footing as the current global PDF fits.

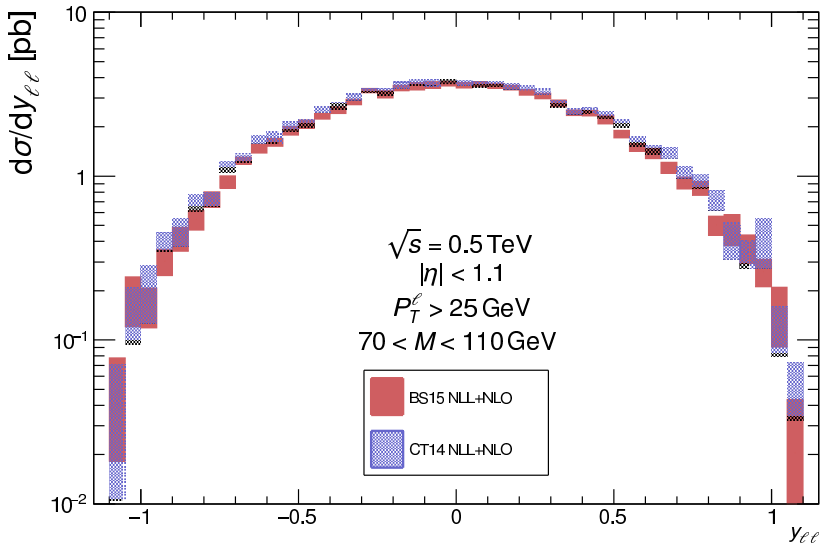

Figure 6: The differential cross section for DY-pair $Z/\gamma^* \to l\bar{l}$ production, versus dilepton rapidity, with the cuts corresponding to the acceptance of the STAR detector. The predictions use the BS15 and CT14 PDF models, for comparison.

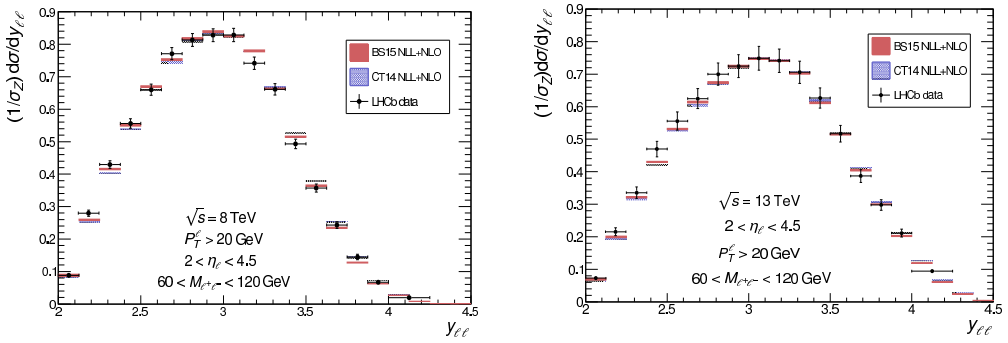

Figure 7: The normalized differential cross section for the forward DY-pair $Z/\gamma^* \to l\bar{l}$ production as a function of dilepton rapidity, at $\sqrt{s} = 8$ TeV (left) [21] and at $\sqrt{s} = 13$ TeV (right) [22]. The experimental data are compared to the predictions using the BS15 and CT14 PDF models.

Acknowledgments The authors would like to thank M. Posik for helpful correspondence. R. P. was partially supported by the Swedish Research Council, contract number 621-2013-428. E. B. is supported by CAPES and CNPq (Brazil), contract numbers 2362/13-9 and 150674/2015-5.

References

[1] M. L. Mangano, arXiv:1512.00220 [hep-ph].

[2] S. Alioli *et al.*, arXiv:1606.02330 [hep-ph].

[3] E. Basso, V. P. Goncalves, J. Nemchik, R. Pasechnik and M. Sumbera, Phys. Rev. D **93**, no. 3, 034023 (2016).

[4] R. Hamberg, W. L. van Neerven and T. Matsuura, Nucl. Phys. B **359**, 343 (1991) Erratum: [Nucl. Phys. B **644**, 403 (2002)].

[5] A. D. Martin, W. J. Stirling, R. S. Thorne and G. Watt, Eur. Phys. J. C **63**, 189 (2009).

[6] J. C. Peng and J. W. Qiu, Prog. Part. Nucl. Phys. **76**, 43 (2014).

[7] E. Basso, C. Bourrely, R. Pasechnik and J. Soffer, Nucl. Phys. A **948**, 63 (2016).

[8] C. Bourrely and J. Soffer, Nucl. Phys. A **941**, 307 (2015).

[9] C. Bourrely, F. Buccella and J. Soffer, Int. J. Mod. Phys. A **28**, 1350026 (2013).

[10] C. Bourrely, F. Buccella and J. Soffer, Eur. Phys. J. C **23**, 487 (2002).

[11] C. Bourrely, J. Soffer and F. Buccella, Eur. Phys. J. C **41**, 327 (2005).

[12] P. M. Nadolski *et al.*, Phys. Rev. D **78**, 013004 (2008);
J. Pumplin *et al.*, Phys. Rev. D **80**, 014019 (2009);
H. -L. Lai *et al.*, Phys. Rev. D **82**, 074024 (2010).

[13] S. Dulat *et al.*, Phys. Rev. D **93**, 033006 (2016).

[14] S. Catani, D. de Florian, G. Ferrera and M. Grazzini, JHEP **1512**, 047 (2015);
G. Bozzi, S. Catani, G. Ferrera, D. de Florian and M. Grazzini, Phys. Lett. B **696**, 207 (2011).

[15] S. Catani, D. de Florian and M. Grazzini, Nucl. Phys. B **596**, 299 (2001).

[16] J. M. Campbell and R. K. Ellis, Phys. Rev. D **60**, 113006 (1999).

[17] J. Campbell, R. K. Ellis, *MCFM - Monte Carlo for FeMtobarn processes*, `http://mcfm.fnal.gov`.

[18] S. Catani, L. Cieri, G. Ferrera, D. de Florian, M. Grazzini, Phys. Rev. Lett. **103** 082001 (2009);
S. Catani, M. Grazzini, Phys. Rev. Lett. **98** 222002 (2007).

[19] M. Posik *et al.* [STAR Collaboration], PoS DIS2015, 051 (2015).

[20] V. Khachatryan *et al.* [CMS Collaboration], Eur. Phys. J. C **76**, no. 8, 469 (2016).

[21] R. Aaij *et al.* [LHCb Collaboration], JHEP **1601**, 155 (2016).

[22] R. Aaij *et al.* [LHCb Collaboration], JHEP **1609**, 136 (2016).